# TECHNICAL PAPER

# How Clean is Clean: Non-Destructive/Direct Methods of Flux Residue Detection

***By*** Mark Koch, Brian R. Stallard, Randall D. Watkins, Mary M. Moya
Sandia National Laboratories
Christopher W. Welch
College of William & Mary
Urmi Ray, AT&T Bell Laboratories
Princeton, NJ

**International Conference on Solder Fluxes and Pastes**

***Presented at*** **Georgia Institute of Technology Atlanta, Georgia**

June 1-3, 1994

**CONFERENCE SPONSORS**

Institute for Interconnecting and Packaging Electronic Circuits

School of Materials Science and Engineering
Georgia Institute of Technology

Published by IPC

7380 N. Lincoln Ave.
Lincolnwood, Illinois
60646-1705
Tel 708 677-2850
Fax 708 677-9570

# How Clean is Clean: Non-destructive/Direct Methods of Flux, Residue Detection

*By: Christopher S. Welch (College of William & Mary), Urmi Ray (AT&T Bell Laboratories), Brian R. Stallard, Randall D. Watkins, Mark W. Koch and Mary M. Moya (Sandia National Laboratory)*

## 1. Inspection needs for printed circuit board manufacturing.

With a new generation of fluxing, soldering and cleaning technologies in the electronic industry, the entire assembly process needs to be reevaluated from a yield, quality and reliability perspective. From the standpoint of long-term reliability, it is important to distinguish between innocent chemical residues and "dangerous" ones. Cleanliness detection methods, of course, change with the use of new solder fluxes and pastes. Several on-line detection methods popular in the rosin flux/CFC cleaning era have become questionable in the emerging technologies using "no-clean", or low solids flux soldering.

In 1992, a team was formed under the umbrella of the National Center for Manufacturing Sciences (NCMS) to establish a correlation between the type and quantity of residues left on a printed circuit board (PCB) and the electrical performance of a circuit. The goal was to perform analyses of specific chemical residues and establish the impact of these chemical residues on electrical function. The guiding principle used is that contamination induced failure occurs when a chemical concentration exceeds a critical value.

In order to maintain consistency in the study, two important issues were addressed for the study. First, model fluxes were used to avoid variables (such as extraneous additives) associated with using commercial fluxes. Second, contamination-by-design was used, so dose-response curves were generated by using specimens that were contaminated with "controlled" amounts of specific chemicals.

Theoretically, analysis of the "type" and "quantity" of the contaminants can be done in one of the two ways.

I) *Direct analysis of residue on substrate.* This is the "ideal" way of measuring cleanliness. An electronic assembly operation almost always results in uneven distribution of flux/solder residues over the PCB area. In general, areas near or underneath large components are harder to clean. Concentration of "harmful" residues across conductor lines will be harmful to the electrical performance of the circuit board. Therefore, the group considered it necessary to research available techniques for direct analyses of residues on PCB's. Three techniques were investigated: Optically Stimulated Electron Emission (OSEE), Fourier Transform Infrared Spectroscopy (FTIR), and Optical Imaging. The detection limits and the advantages and disadvantages of each technique are described respectively in sections 2,3 and 4. Most of the work on

"direct" analysis are preliminary, and studies are ongoing to improve the detection methods.

Preliminary feasibility studies using OSEE were completed for detecting rosin flux residue on FR-4 (insulator) substrates. The detection method was significantly modified to obtain reproducible results from FR-4. After establishing the baseline reproducibility, a dose-response curve with Rosin Mildly Activated (RMA) flux was generated, demonstrating the sensitivity of this detection technique in the 0-10 $\mu g/cm^2$ range. Further work on detecting low solids flux residues and to make the technique more rugged and suitable for use in a manufacturing environment is ongoing.

FTIR microscopy was able to track relative changes in residue levels from rosin based, low-solids and water soluble flux as a function of processing conditions (i.e., soldering and cleaning). There are two fundamental problems with using FTIR microscopy as a process monitoring tool: (a) lack of sensitivity at low concentrations and (b) inability to discriminate organic residues (such as flux) from the organic (FR-4) substrates.

Optical imaging studies using sophisticated image processing algorithms demonstrated the viability of using this technique when relatively high concentrations of flux residue are present on the board surface. At lower levels, which are more typical of standard wave soldering operations, alternate sensor techniques need to be developed or higher image magnifications need to be attained. A method for multiple point analyses over the entire area of the circuit board might be necessary. Image analysis has proved to be useful in identifying small amounts of potentially "dangerous" chemicals against a visual background that contains massive amounts of adipic acid. However, that would require analysis of high magnification images, which precludes its implementation as an end-of-line quality control tool. Future work in image analysis will focus on tools for characterizing contamination and failure mechanisms in the laboratory.

Some other direct methods of great utility in surface science were also considered, including X-Ray Photoelectric Spectroscopy (XPS), Auger Electron Spectroscopy (AES) and blacklight inspection. These were not considered suitable for PCB inspection because of factors such as requirements for an ultra high vacuum system, lack of sensitivity, and other limiting requirements of the techniques.

II) *Extraction based Analysis:* The most common and universally accepted analytical methods for residue detection on electronic assemblies are all based on extraction. These methods depend on optimizing an extraction method for removing the residue from the PCB substrate, followed by analysis of the extract. All extraction based methods provide an average over the entire area of the circuit board. So far, two extraction based detection methods were investigated by the group: Ion Chromatography (IC) and Solvent Extract Conductivity (SEC). An optimum method of extracting and detecting low solids flux residues was developed by this team through extensive round robin testing [Ray, et al, 1994].

## 2. Optically Stimulated Electron Emission (OSEE)

OSEE is a technique used for inspecting surfaces for contamination. It has been of restricted use in some specialty areas, in which it has generally been successful owing to its ease of application, rapidity of response and simplicity of interpretation. It has not had wider use because in some instances it is highly variable and difficult to interpret. Its uses have been mostly as a quality control indicator in production environments where the sources of contamination are few and reproducible and the inspection surfaces are primarily metals. The work reported here represents an extension in the application of OSEE.

### 2.1. Descriptive introduction to OSEE

Optically Stimulated Electron Emission (OSEE) is a measurement which is based on the photoelectric effect, in which a photon of light with a sufficiently short wavelength, or high energy, interacts with the materials constituents of the solid surface it strikes to eject an electron [Smith 1975, 1979]. These so-called photoelectrons can be detected with sufficiently sensitive electrometers if they are collected on a positively charged anode. A schematic of OSEE as used for inspection of Shuttle Solid Rocket Motor casing is shown in Figure 2.1 [Gause, 1989]. The essential elements in the OSEE measurement process are shown as a light source, a positively biased electrode connected through an electrometer, and a conductive return path to return charge to the sample equivalent to that removed.

In previous work [Welch, et al., 1991; Welch, et al., 1992], it has been shown that the field strength at the sample surface is an important determinant of OSEE current, although currents are generally low enough that field modification by the photoelectrons, the space charge effect, is not substantial. With a low pressure mercury discharge lamp, it has been shown that the very short (185 nm) component in the illumination is responsible for the majority (~95%) of the OSEE current observed. This wavelength is known to interact with atmospheric oxygen to produce ozone, which is frequently detectable by its odor near an OSEE measurement apparatus. It is also known to interact with water vapor. The resulting reaction products are themselves highly reactive, and engage readily in surface chemistry with the sample, changing surface characteristics including OSEE current generation capacity. These tendencies lead to variability in the OSEE current from the sample which is not related to the initial surface condition. This variability sometimes obscures the interpretation of OSEE data. Previous work has shown this variability to be largely suppressed by purging the illuminated volume of an OSEE measurement with argon gas, which is non-reactive. The intensity of short wave radiation emitted from a low pressure mercury arc lamp is dependent on lamp current and bulb temperature. Once these interferences and sources of variability are taken into account, the OSEE measurement of a given surface gains both reproducibility and stability.

The OSEE measurement from a given substrate has been shown to be sensitive to very small amounts of some contaminants, in particular oils and greases. Previous work has

shown that part of the sensitivity is due to absorption of the incident light by the contaminant. Many organic compounds have a very high absorptivity to light at 185 nm. Some other compounds and mixtures become photoconductors under ultraviolet radiation. For these, an alteration of the work function of the surface occurs increasing the sensitivity of OSEE to contamination at very low levels. In summary, previous work on metallic substrates has shown OSEE to be a sensitive indicator of small amounts of contamination on metal substrates. In any particular case, pending a general theory of OSEE response, it necessary to develop a dose-response curve for each new contamination-substrate combination for which contamination monitoring is desired.

## 2.2. Application of OSEE to Circuit Board Inspection

To apply OSEE to printed circuit board inspection, several issues must be considered. First, the substrate consists of two types of surfaces, a soldered copper surface and an insulating surface. Second, the contaminant should be a known substance. In the case of circuit boards, the contaminant is solder flux, a known substance in each particular production system. The response of OSEE on soldered copper is shown in Figure 2.2, which depicts three successive measurement runs on each of two samples in a laboratory environment. The data suggest that the state of a clean surface is indicated by an OSEE current in a range of 10% of the reading on the initial exposure to illumination. This provides the first indication of measurement reproducibility needed to produce a viable inspection on soldered surfaces. The stability of the initial indication, obtained in 5 seconds with the equipment used, suggests that an OSEE inspection system can be made to produce rapid inspections on a production line and so be a practical inspection tool.

## 2.3. Extension of OSEE method to include insulating surfaces.

Virtually all previously reported work on OSEE response is associated with metallic surfaces, for which a reference state of electrical potential can be established with a simple return wire from the sample to the instrument, completing the electrical circuit. With an insulator, no such reference is readily available; yet casual observation with the commercially available OSEE instrument often indicates that OSEE currents are generated when the probe is moved into proximity with an insulating surface. If there is a current produced, there is some hope of producing a viable contamination measurement.

Figure 2.3a shows the results of three successive OSEE measurements on FR-4, an insulating substrate in common use in printed circuit boards. Not surprising, the OSEE current decreases in each run with time. This can be attributed to a decrease in the population of accessible electrons in the illuminated region as those available are removed from the system. The surface also is left with a net positive charge, decreasing the filed in the measurement region. With a good insulator, the charge partly remains on the surface between runs, so that the measured OSEE current depends on the surface charge at the beginning of a measurement. This lack of

reproducibility affects the credibility of the entire measurement, rendering OSEE as generally practiced an impractical contamination measurement tool on insulators.

Examining the OSEE process, the only feature which seems to be missing on insulating surfaces is the return of charges which have been removed by the measurement. Accordingly, for the circuit board case, a substitute method was used to replace the charges. The method, which is termed charge replacement, consists of measuring the total charge which passes through the electrometer during the measurement, and reversing the bias field following the measurement. This reversal generally produces some current in the opposite direction. The current is permitted to flow until an amount of charge has passed the electrometer equal to that which passed the electrometer during the measurement. The measurement is then repeated. The presumption is that the charges passing the electrometer during the reversal find the correct places on the surface by the attraction of the residual positive charge centers following the original removal of the charges.

Examining insulating surfaces, it was shown that the currents require the ultraviolet illumination, that the process acts as a diode, primarily attracting released negative charges, and that the 185 nm line of the lamp spectrum produces the majority of the current. In these regards the insulating surface acted much as a metal surface does. By employing charge replacement, reproducible OSEE runs were attained, as shown in Fig. 2.3b.

2.4. OSEE Dose-Response curve for Rosin Flux on an insulator.

With reproducibility established on a clean surface, the next step is to examine the effect of flux contamination on the insulating surface. This is done in Figure 2.4, which shows three successive measurements using charge replacement on FR-4 substrates with three levels of contamination by rosin flux, the three levels being characterized as none, light and heavy contamination. The runs with charge replacement all show good reproducibility. The initial value of OSEE response decreases as contamination is increased, and the slope of the curve with time also decreases, the highly contaminated case actually responding like a conductor, with essentially no decrease over time. Either the initial value or the slope with time seems to be a good indicator of contamination in these three cases. Because of rapidity of response is desirable in a measurement, the initial response level is chosen as a contamination indicator. Figure 2.5 shows an experimentally determined dose-response curve for rosin flux on FR-4 with the initial reading being used as the response indicator. The general character of the curve, with a rapid decrease in the vicinity of 0-15 $\mu g/cm^2$ and a flat, non-zero response increasing slightly at large contamination levels is similar to the dose-response curve seen on solid rocket motor inspections. It shows that OSEE is an effective contamination monitoring tool for the substrate/contaminant pair in the region of 0-15 $\mu g/cm^2$.

### 2.5 OSEE Inspection Status

The work to date has demonstrated that OSEE is reproducible on soldered copper substrates. It has extended the applicability of OSEE by virtue of establishing reproducibility of successive measurements to the non-conducting FR-4 substrate. It has also identified a contamination level range over which OSEE discriminates contamination amounts, while at larger contamination amounts, it simply indicates heavy contamination. The next step in producing a viable inspection tool is to develop a method to examine a surface composed of soldered copper traces on an FR-4 substrate. Also, contamination by other flux materials should be done. In this effort, it is fortunate that the OSEE current from a soldered surface is nearly the same as the initial current from the substrate alone.

## 3. FTIR Spectroscopy

### 3.1 Introduction

This section describes the evaluation of FTIR spectroscopy for semi-quantitative analysis of flux residues on PCBs. The experiments were conducted for three classes of flux: rosin, low solids, and water soluble. Samples were analyzed to determine the relative amount of residue remaining at various points in the processing. Information was also sought regarding the chemical nature of the residues.

### 3.2 Experimental

Three fluxes were used in these experiments: 1) Alpha 611, a commercial rosin flux, 2) a 1% solution of adipic acid in isopropanol (IPA), which is representative of no-clean or low solids fluxes, and 3) a 10% solution of polyethylene glycol (PEG) in IPA, which is representative of water soluble fluxes. The PEG had a molecular weight of 600. The fluxes were applied to two inch square coupons (FR-4 substrate with copper pads) in measured amounts of either 50 or 250 μl. The solvent was then allowed to evaporate. The coupons were preheated, put through a standard wave soldering process, and cleaned. The types of cleans are described in the appropriate part of the results section. Representative coupons were held back at each step of the processing for FTIR analysis at a later date. The sample preparation was performed at AT&T Bell Labs.

After receipt of the coupons at Sandia National Laboratories, mid-infrared spectra were obtained on a Nicolet 800 FTIR instrument that is equipped with an IR-Plan microscope from Spectra-Tech. The microscope was operated in reflection mode with a beam size of about 500 μm. Each spectrum is the average of 500 scans which represents about a two minute acquisition time. The spectral resolution was 8 $cm^{-1}$. Due to the interference of the organic constituents of the FR-4 substrate, successful detection of flux residue was only possible on the copper pads of the coupons. Single-beam background spectra were acquired using the copper area of virgin coupons. Each

sample was analyzed at multiple points to compensate for possible non-uniform coverage.

## 3.3 Results and Discussion

Fig. 3.1 shows three representative FTIR spectra obtained in the rosin flux experiments. Part A is for the coupon after preheating; part B is for the coupon after wave soldering; and part C is for the coupon after cleaning. Fig. 3.1B is recognizable as the natural product, pine rosin acids, which is the solids portion of most commercial products. The spectral changes from Fig. 3.1A to B are a result of the evaporation of high molecular weight alcohols and esters during the wave solder process.

The narrow lines evident in Fig. 3.1C at 3600 and 1600 $cm^{-1}$ are due to water vapor absorption in the bean path of the spectrometer. Likewise, the unresolved $CO_2$ bands can be seen at 2300 $cm^{-1}$. The broad hump centered at 1600 $cm^{-1}$ has no significance since the baseline of a spectrum is rarely perfectly flat when the absorbance scale is expanded. For trace detection of hydrocarbons it is usual to consider the CH stretch region from 2800 to 3000 $cm^{-1}$. A peak in this region is an unambiguous indication of hydrocarbons. Also, small signals are not obscured by the atmospheric interferences mentioned above.

Two types of cleans were used for the rosin flux: 1) terpene, and 2) freon/TMS. Both left an undetectable amount of hydrocarbons on the copper pads, as seen in Fig. 3.1C. The noise level is about 4 $x10^{-4}$ absorbance units in the CH region. Given absorbances of about 0.5 units in Figs. 3.1A and B, less than about 0.2% of the original material was left on the pads after cleaning. In this estimate we assume that a signal-to-noise ratio of 2.5 is sufficient for detection. Longer signal acquisition times and the use of mutlivariate spectral analysis could improve this detection limit, if required.

Figs. 3.2 and 3.3 show representative spectra obtained in the adipic acid flux experiments. The results are somewhat different for batch #1 and batch #2 which are associated with Figs. 3.2 and 3.3, respectively. A third batch of samples produced spectra equivalent to Fig. 3.2. The differences cannot be explained by any known change in the sample preparation. For Fig. 3.2, part A is a transmission spectrum of pure adipic acid; part B is for the as-coated coupon; and part C is for the coupon after cleaning. The spectrum after wave soldering (not shown) has the same shape as in Fig. 3.2B, with about half the absorption intensity. This, of course, is an indication that about half the material is removed by the wave soldering step. The cleaning step for adipic acid flux is accomplished with IPA/$H_2O$. There is approximately 2% of the material remaining after the clean, as judged by the height of the CH peak at about 2900 $cm^{-1}$ in Fig. 3.2C. Note that the material remaining after the clean is not adipic acid but principally a chemical with a prominent band at 1585 $cm^{-1}$ (noted by the stars in Fig. 3.2). This may be an impurity in the adipic acid preparation or more probably a metallic ester formed by reaction with the copper surface.

Fig. 3.3 show two representative FTIR spectra obtained in the adipic acid flux experiments, batch #2. Part A is for the coupon after preheating; and part B is for the coupon after wave soldering. No cleaning was done on this batch. Interestingly, the wave soldering step alone removed essentially all the adipic acid, unlike batch #1, where about half was removed. After the wave soldering step, only the metallic ester remains (as we have tentatively identified the chemically changed material). Curiously, the residues in Figs. 3.2C and 3.3B are not precisely the same, since the starred peak is shifted from 1585 $cm^{-1}$ in Fig. 3.2C to 1511 $cm^{-1}$ in Fig. 3.3B. The cause of this shift is unknown. Finally, the broad band peaking at 750 $cm^{-1}$ is a bit large to be disregarded as an instrument artifact. Low frequency, broad bands are usually associated with inorganic compounds. No positive identification can be made. Based on the spectral evidence that: 1) more material is removed, and 2) more material is converted to metallic ester; we speculate that the samples in batch #2 accidentally saw a higher temperature during wave soldering step.

An important observation relating to Figs. 3.2 and 3.3 is that the shape of the prominent peak at about 1700 $cm^{-1}$ is different in the reflection spectra as compared to the transmission spectrum (Fig. 3.2A). A pure reflection spectrum off the front surface of the flux coating would have a shape something like the first derivative of the transmission absorption band. The fact that there is a dip before the strong peaks in Figs. 3.2B and 3.3A indicates that they contain a small component of reflection. Nevertheless, the principal component of each spectrum is transmission-like because the beam reflects off the copper pad, thus passing through the sample twice. The proportion of reflection versus transmission character in the spectra depends on the reflectivity of the copper and the refractive index of the flux residues. Since these variables are not fixed, a very complicated scheme for pre-processing the spectra would be necessary for the careful quantitative work.

Fig. 3.4 shows three representative spectra obtained in the PEG experiments. Part A is a transmission spectrum of pure PEG; part B is the as-coated coupon; and part C is for the coupon after cleaning. The spectrum of the coupon after wave soldering is not shown since it is not significantly different in intensity or shape from Fig. 3.4B. There is a noticeable tilt to the baseline in Fig. 3.4B which is due to light scattering losses. This is also evident in some of the previous figures. The imperfect baseline in Fig. 3.4C is not significant. In Fig. 3.4B the shape of the peak at about 2900 $cm^{-1}$ seems to be slightly distorted by the reflection phenomenon mentioned above. Also, it is curious, but unexplained, why the low frequency bands are depressed relative to the high frequency bands. The cleaning step seems effective as judged by the disappearance of the CH peak. The clean was accomplished with water at 50 C. In this case, the detection limit, in terms of absorption units, is the same as in fig. 3.1. However, this absorbance represents about 1% of the initial material since the absorbance in Fig. 3.4B is about five times lower than in Fig. 3.1A or B. Having examined a number of coupons at a number of locations, we found a few points with detectable CH peaks after cleaning. Therefore, this cleaning process probably produces coupons with residues only slightly below the detection limit, on average.

One unexplained result requires mentioning. Many of the above experiments were repeated with nominal loadings of both 50 and 250 μl of flux. Surprisingly, the as-coated spectra did not show a statistically significant absorbance difference between the two loadings.

### 3.4 Conclusions

A principal limitation of FTIR spectroscopy is that it can only detect flux residues on the copper areas of PCBs. Also, due to the reflectance versus transmission problem, it is difficult to obtain a high degree of accuracy and linearity in the quantitative determination of flux residues. Nevertheless, FTIR spectroscopy clearly provides useful information. The sensitivity of a standard commercial instrument allows one to follow the flux removal down to about 1% of the original loading. Improvements can be contemplated to improve this detection limit by about 3 to 5 times. Creating a scanning imaging of impurities with an FTIR microscope is possible, in principle, but will be very time consuming when operating near the detection limit. A notable strength of FTIR spectroscopy is that the spectra contain considerable chemical information. When questions of chemical changes during processing arise, FTIR spectroscopy can be a valuable tool.

Finally, we summarize the flux cleaning results. Traditional cleans for rosin fluxes are very effective, removing the flux to less than about 0.2% of the original loading. Adipic acid flux residues are removed to a variable degree (at least 50%) by the wave soldering process and can be further removed to the 2% level with additional IPA/$H_2O$ cleaning. The tenacious hydrocarbon remaining after use of the adipic acid flux is probably a metallic ester. PEG fluxes are hardly affected by the wave soldering process and removed to less than about 1% with heated water.

## 4. Optical Imaging with Image Analysis

Video imagers have become small, available and easy to employ over the last several years, and the field of machine vision coupling video imagers with digitizers is growing and is a logical candidate for analysis of PCB's. A demonstration effort was used to illustrate how these powerful elements can be used to inspect for residues of adipic acid, which forms light-colored crystalline patterns on PCB's. The inspection technique retains the visual impact and archivability of a photograph while permitting inspections to be done automatically through use of a Residue Detection Algorithm (RDA). Because it was desirable for algorithm development to maintain the samples in a stable manner, sodium chloride, which forms residues similar to adipic acid, was used for the demonstration.

The first step was to form an image which produces high contrast between a clean substrate and one with residues present. In practice, the full array of gating, polarizing, filtering and fluorescence techniques are available to an inspection for producing this image. Because the image analysis techniques and automatic RDA building process were the new technology under examination, oblique lighting was used in this effort.

Figure 4.1 shows a video image of sodium chloride residue on a PCB at a resolution of 38 pixels per millimeter. For a given video imager, lower resolutions permit single frame analysis to cover larger areas, while high resolutions show detailed crystal shapes and detect contamination residues at concentrations of less than 100 micrograms per square inch. In the image, the substrate appears gray with some visible structure, the circuit traces appear black due to specular reflection, and the crystalline residues appear as distinct bright regions on their local background. Less apparent to the visual inspection is an intensity gradient across the entire image due to the oblique lighting. The large contrast between the traces and the substrate as well as the lighting gradient, while easily discriminated against by human visual inspection, prevent an automated analysis by simple threshold or edge detection methods and require the development of a more sophisticated RDA. The following discussion describes the RDA developed for this inspection and the results of applying it to the images of PCB residue.

Figure 4.2 shows the block diagram of the RDA, with an inset graph showing a one-dimensional (1D) cross-section of the two-dimensional (2D) result of each process in the RDA. The input cross-section shows the traces appearing as deep wells in the signal, which mostly appears otherwise as a sloped line from the intensity gradient. The residue appears as small signal peaks above both the sloped line and the traces.

The human visual system follows a Weber Law, which describes how the just-noticeable difference depends on the background. Brighter backgrounds correspond to larger just-noticeable differences. The feature contour shunting network also implements a Weber Law.

We implement these Weber Laws by approximating the average background level of the fill network output. For the inverted law, we replace the average background level with the eroded [Marangos and Shafer, 1990] binary fill output. This denominator acts like a mask that inhibits response on the dark traces. For the strong law, we replace the average back ground level with an eroded negated binary fill output. Here, the virtual mask inhibits response on the bright substrate. In both cases, the erosion process inhibits the trace edge response.

For more details on equations and parameters for the RDA algorithm, see reference [Koch and Moya, 1993].

## 4.3 Results

Figure 4.3 shows a PCB residue image and the output image of the algorithm. The normalized average residue surface volume in Figure 4.3 is 24. Since the algorithm also detects substrate defects, the value for a clean board is 13.

## 4.4 Conclusions

We have developed an automatic residue detection system for detecting light colored crystalline residue on printed circuit boards. Using 38 pixels/mm magnification and

oblique lighting, we can enhance the residue's macroscopic properties. BCS/FCS removes the illumination gradient and allows the use of Weber normalization to detect microscopic residues on the substrate and traces.

In our work to develop an automatic residue detection system, we discovered that even high concentrations of residue are barely visible in a low magnification visual image. We were able to develop an automatic visual system that detects high concentrations of light-colored crystalline residue.

Future work will focus either on processing of images created by alternate sensing techniques or on developing a visual pattern recognition system for high magnification images that could facilitate laboratory investigation of the relationship between contamination residues and electrical performance.

## 5. Conclusion

The feasibility of three different non-destructive and direct methods of evaluating PCB cleanliness was demonstrated. The detection limits associated with each method were established. In addition, the pros and cons of these methods as routine quality control inspection tools were discussed. OSEE was demonstrated to be a sensitive technique for detection of low levels of flux residues on insulating substances. However, future work including development of rugged OSEE instrumentation will determine whether the PCB industry can accept this technique in a production environment. FTIR microscopy is a well established technique with well known characteristics. The inability of FTIR to discriminate an organic contaminant from organic substrate limits its usefulness as a PCB line inspection tool, but it will still remain a technique for the QC/QA laboratory. One advantage of FTIR over the other two techniques described here is its ability to identify the chemical nature of the residue, which is important in Failure Mode Analysis. Optical imaging using sophisticated pattern recognition algorithms was found to be limited to high concentrations of residue.

Further work on improved sensor techniques is necessary.

## 6. Acknowledgements

The authors gratefully acknowledge the support and sponsorship of the National Center for Manufacturing Science, without which we would never have met, let alone worked together. In this regard, Clare Vinton and Mike Wixom have been particularly helpful. The "How Clean is Clean" team have worked well together, sharing information, samples and other necessaries. These include Carol Ellenberger of Texas Instruments, John Sohn of AT&T, Brenda Schubert and Vicki Heideman of GM Delco, Jerry Rosser of GM Hughes, and Karen Adams and Jim Anderson of Ford. Steve Lehrman of Research Triangle Institute and Frank Farmer at NASA Langley Research Center were instrumental in making the OSEE work a part of this project, and the OSEE laboratory work was ably handled by Xuaco Pascual of AS&M, Inc. W.T. Yost of NASA Langley provided encouragement and advice as well as laboratory access.

## 7. References

Gause, Raymond L. A noncontacting scanning photoelectron emission technique for bonding surface cleanliness inspection, NASA TM-100361 February 1989, 53pp.

M. Koch and M. Moya, Detecting residue on a printed circuit board: an application of the Boundary Contour/Feature Contour System, to appear in World Congress on Neural Networks, Portland OR, July 1993.

P. Marangos and R. Schafer, Morphological Systems for Multidimensional Signal Processing, Proceedings of the IEEE 78 (4) : 690-710, April 1990.

Ray, U., J. E. Sohn, S. Toll, V. Heideman, M. Young, K. Adams and Y. Graves, How clean is clean: Optimization of extraction/ion chromatography parameters for no-clean flux residue detection, presented at the International Conference on Solder Fluxes and Pastes, Atlanta, GA., June 1-3, 1994.

Smith, Tennyson, Photoelectron emission from aluminum and nickel measured in air, J. Appl. Phys. 46(4), p. 1533, (1975).

Smith, Tennyson, Quantitative techniques for monitoring surface contamination, in Mittal, ed., Surface Contamination – Genesis, Detection and Control, Plenum Press, New York, pp 697-712, (1979).

Welch, C. S., W. T. Yost and M. N. Abedin, OSEE inspection of solid rocket motor steel, Proc. Of the Third Conference on NDE for Aerospace requirements, Huntsville, AL, June 4-6, 1991. pp. 200-237.

Welch, C. S., M. N. Abedin and W.T. Yost, Optically stimulated electron emission: Current-voltage response and spectral sensitivity, Review of Progress in Quantitative Nondestructive Evaluation, Vol. 11, D. O. Thompson and D. E. Chimenti, eds, Plenum Press, New York, 1992.

*Welch, et al: List of Figures*

Fig. 2.1. – Schematic diagram of OSEE contamination monitoring system applied in Space Shuttle inspections. Elements shown of an OSEE measurement include an ultraviolet lamp illuminating the surface under inspection, a biased electrode to collect negatively charged emissions, an electrometer to monitor the resulting current and a conducting return path to complete the circuit.

Fig. 2.2 – OSEE current vs. time on two clean soldered copper surfaces. Surfaces are exposed to light from 50 seconds in the run to 450 seconds. Three repetitions are shown for each surface.

Fig. 2.3 – OSEE current vs. time on an insulating (FR-4) surface with three repeated measurements. In a), sequential measurements were used with a recovery period between measurement sets. In b), charge replacement was used between measurements. The data clearly show better reproducibility with charge replacement.

Fig. 2.4 – OSEE current vs. time on an insulating (FR-4) surface with three contaminant levels: a) no contaminant, b) little contaminant and c) heavy contaminant layer. The sequence shows a successive lowering of the initial OSEE current as well as a decrease in the rate of time variability with increasing contamination.

Fig. 2.5 – dose-response measurements of Alpha 611 Rosin Flux on an FR-4 substrate. These measurements, which form a consistent trend line, were obtained from three different substrates, indicating that the curve is generic to the substrate-contaminant pair rather than specific to the particular samples tested.

Fig 3.1 – FTIR spectra from the coupons processed with rosin flux. Spectrum A is after preheating; B is after wave soldering; and C is after cleaning. The spectra are offset with each origin indicated by a zero along the y-axis. The relative expansion for each spectrum is indicated following its label. The absorbance scale for a 1 x expansion is 0.25 units per minor tick mark.

Fig. 3.2 – FTIR spectra from the coupons processed with the adipic acid flux, batch #1. Spectrum A is a reference transmission spectrum; B is as-coated; and C is after cleaning. The spectra are offset with each origin indicated by a zero along the y-axis. The relative expansion for each spectrum is indicated following its label. The absorbance scale for a 1 x expansion is 0.05 units per minor tick mark. The star indicates a peak at 1585 $cm^{-1}$ that is referred to in the text.

Fig. 3.3 – FTIR spectra from the coupons processed with the adipic acid flux, batch #2. Spectrum A is after preheating, and B is after wave soldering. The spectra are offset with each origin indicated by a zero along the y-axis. The relative expansion for each spectrum is indicated following its label. The absorbance scale is 0.05 units per minor tick mark. The star indicates a peak at 1511 $cm^{-1}$ that is referred to in the text.

Fig. 3.4 – FTIR spectra from the coupons processed with PEG flux. Spectrum A is a reference transmission spectrum of PEG; B is as-coated; and C is after cleaning. The spectrum of the sample after wave soldering is not significantly different from B. The spectra are offset with each origin indicated by a zero along the y-axis. The relative expansion for each spectrum is indicated following its label. The absorbance scale for a 1 x expansion is 0.05 units per minor tick mark.

Fig. 4.1 – Example input image for optical detection of residues.

Fig. 4.2 – Block diagram of approach taken in residue detection algorithm.

Fig. 4.3 – Result of applying the residue detection algorithm to the input image shown in Fig. 4.1.

Figure 2.1

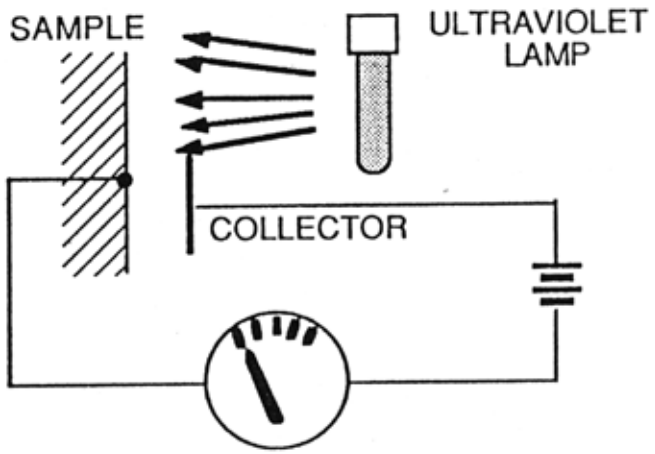


Figure 2.2

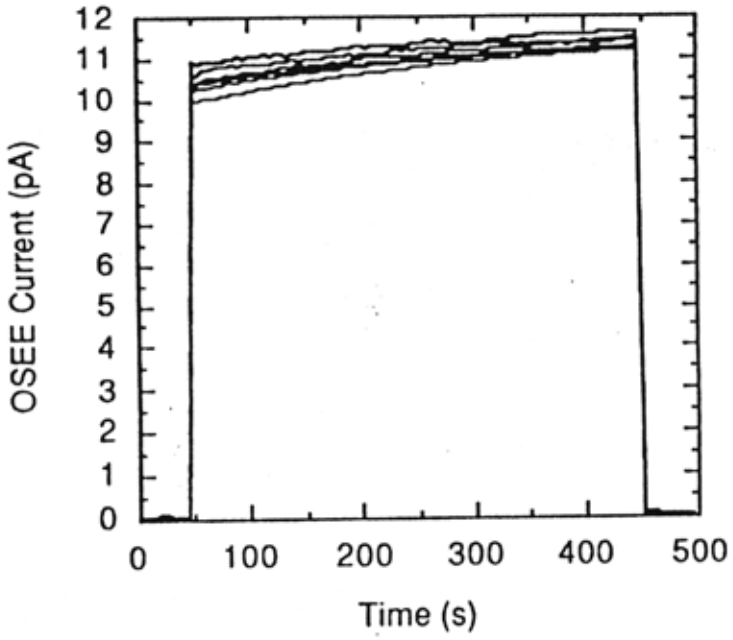

Figure 2.3

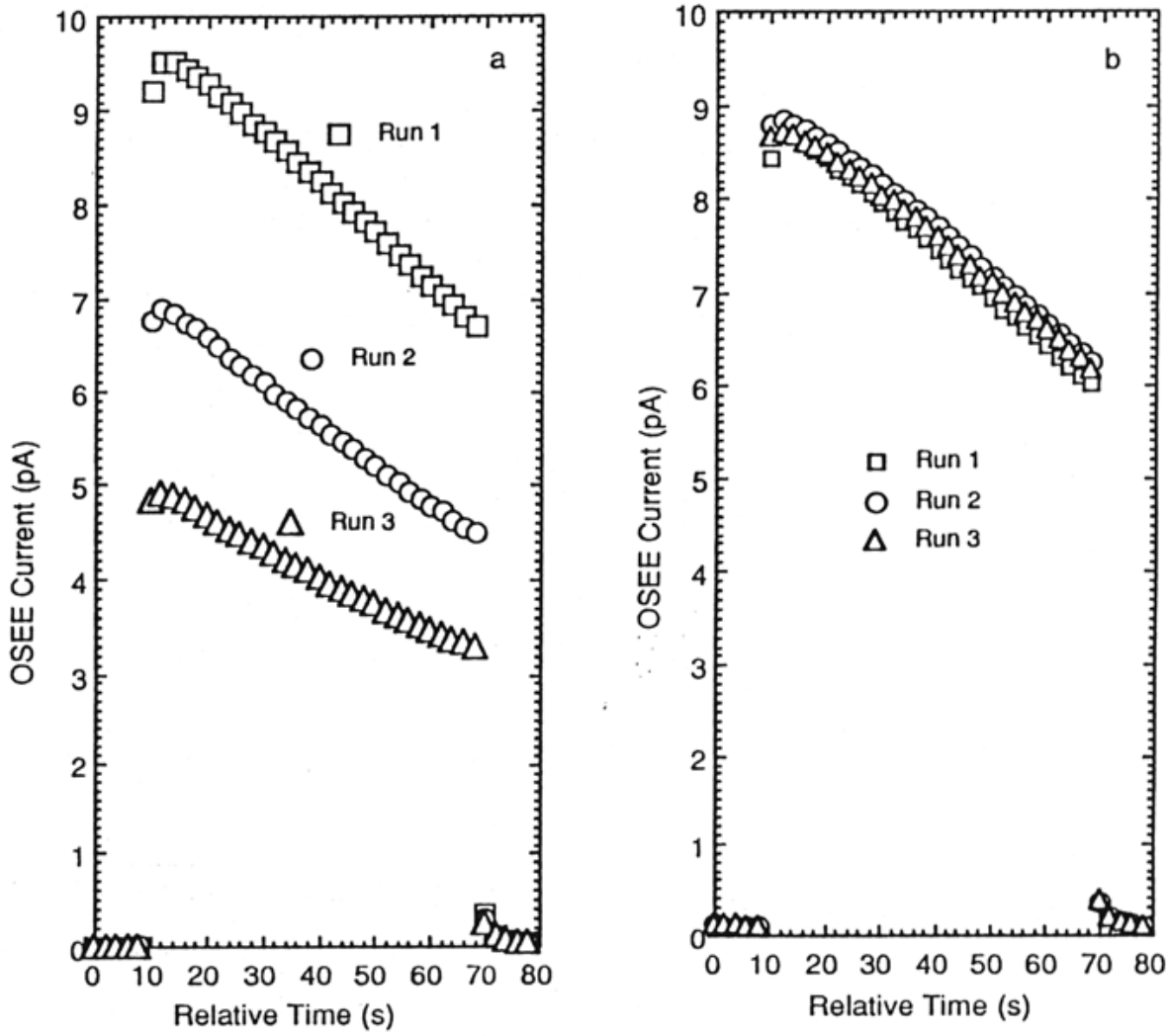
a
Run 1
Run 2
Run 3
OSEE Current (pA)
Relative Time (s)
0 10 20 30 40 50 60 70 80
0 1 2 3 4 5 6 7 8 9 10
b
Run 1
Run 2
Run 3
OSEE Current (pA)
Relative Time (s)
0 10 20 30 40 50 60 70 80
0 1 2 3 4 5 6 7 8 9 10

Figure 2.4

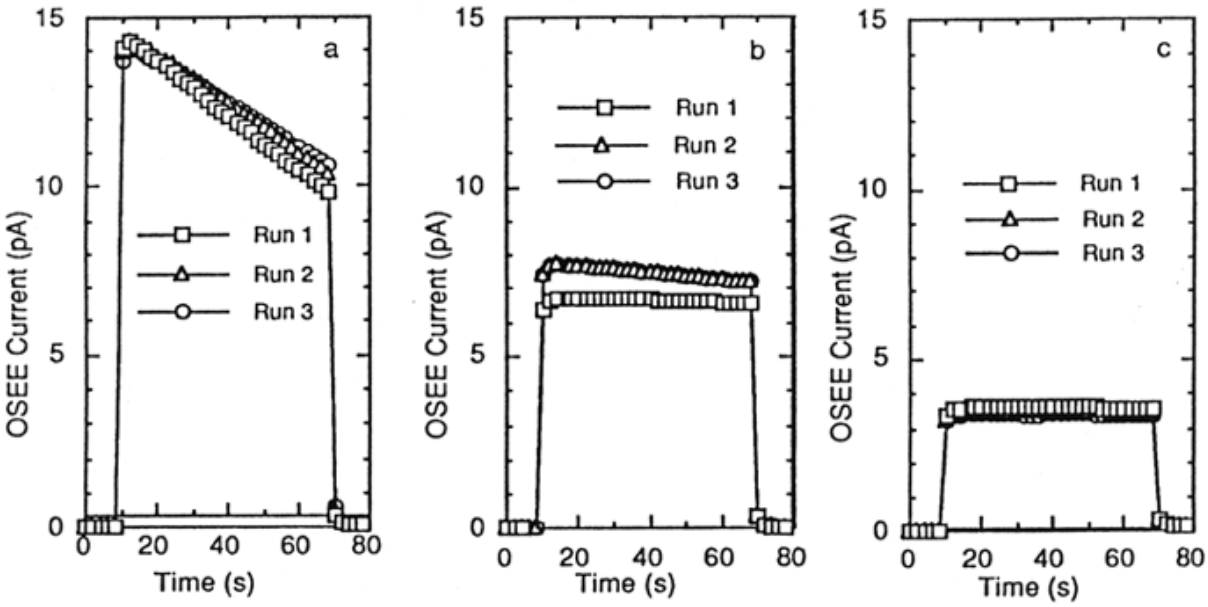


Figure 2.5

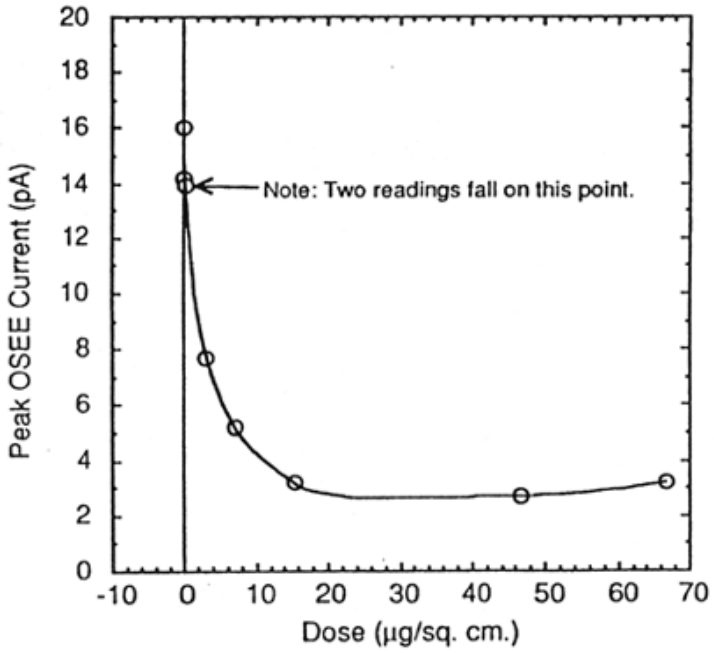

Figure 3.1

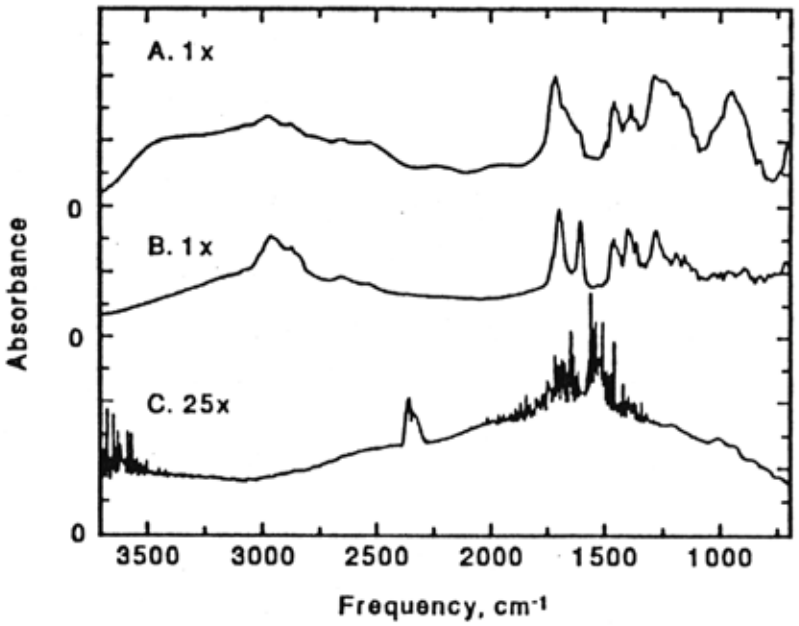


Figure 3.2

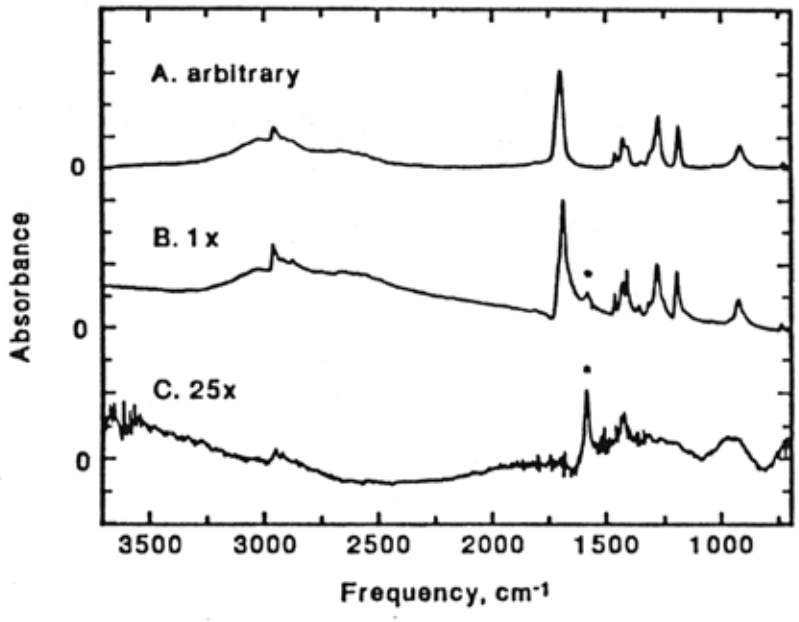

Figure 3.3

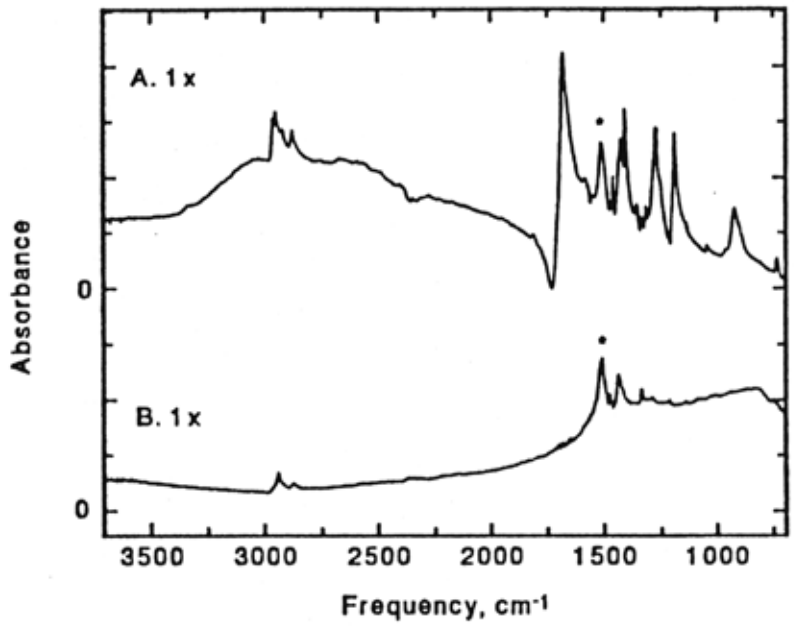


Figure 3.4

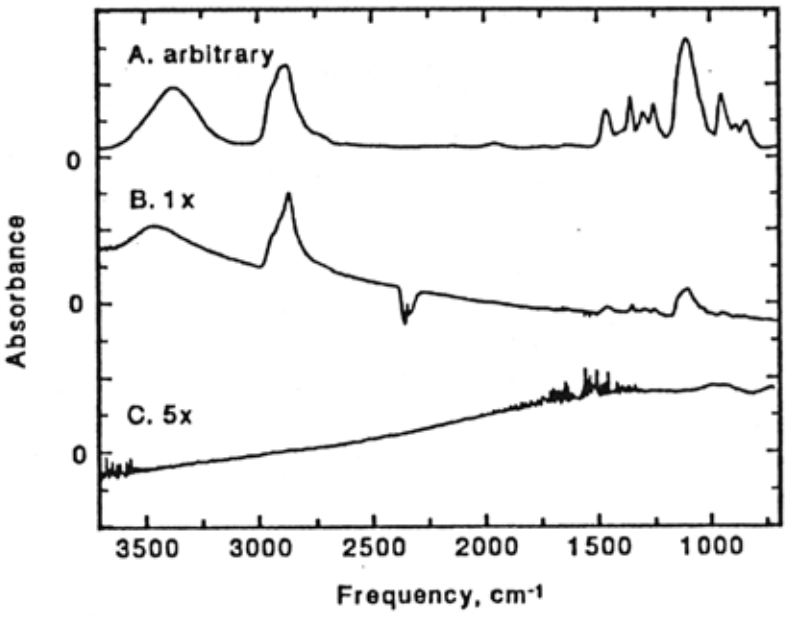

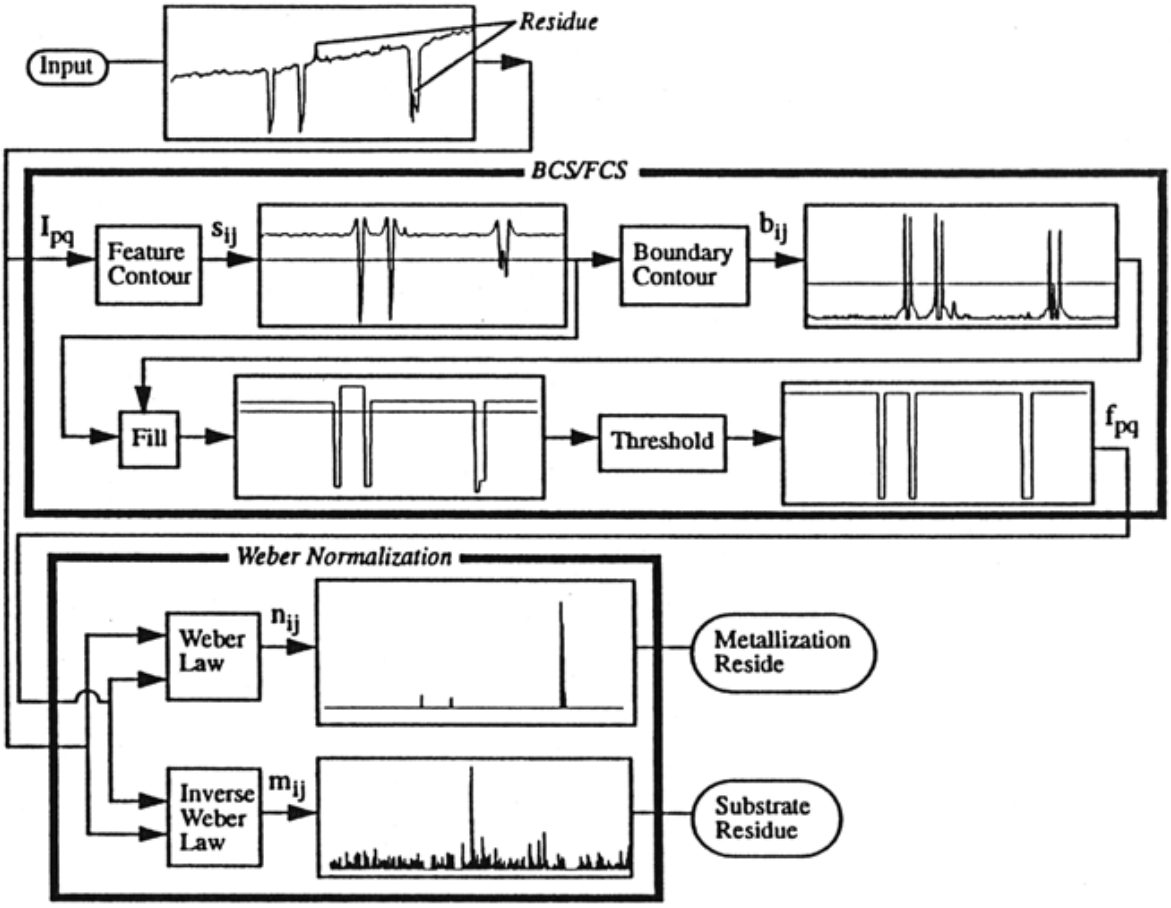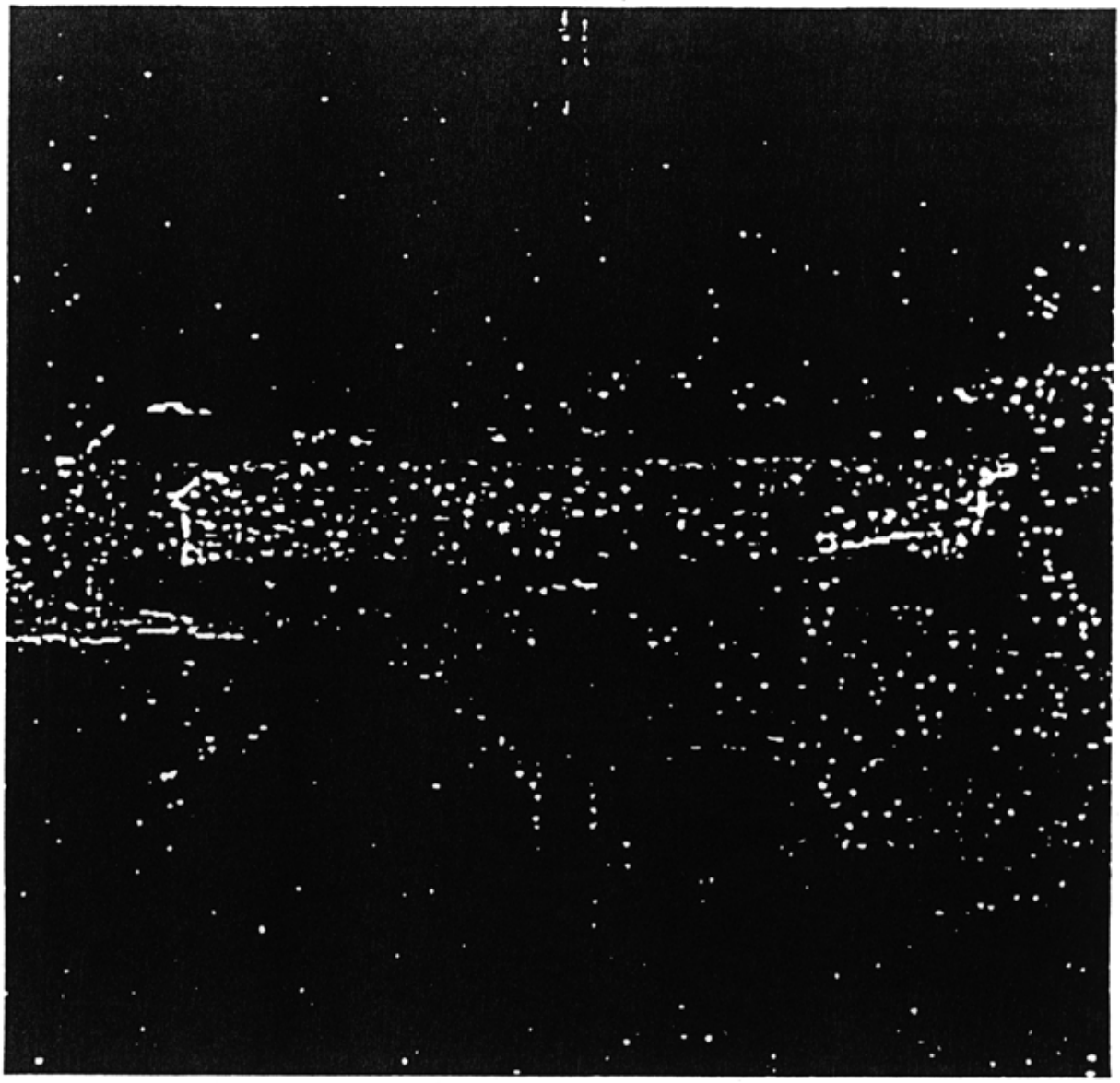
Input
Residue
BCS/FCS
$I_{pq}$
Feature Contour
$s_{ij}$
Boundary Contour
$b_{ij}$
Fill
Threshold
$f_{pq}$
Weber Normalization
Weber Law
$n_{ij}$
Metallization Reside
Inverse Weber Law
$m_{ij}$
Substrate Residue